

# 34. A Hybrid Wide-slot Antenna with Elliptical and Staircase-shaped Wide-slots for Wideband Applications

Munish Kumar<sup>1</sup> and Vandana Nath<sup>2</sup>, University School of Information, Communication and Technology  
GGG Indraprastha University, New Delhi, India  
<sup>1</sup>munishkm1989@gmail.com, <sup>2</sup>vandanausit@gmail.com

## ABSTRACT

Miniaturized antennas having multiband or wideband capability are the need for modern wireless applications. In this paper, a microstrip-line-fed hybrid wide-slot (HWS) antenna of compact size is proposed for wideband applications. The main body of the proposed antenna includes an elliptical wide-slot (EWS) and staircase-shaped rectangular slots merged with each other. This HWS is excited using an open-ended microstrip line having a characteristic impedance of  $50\Omega$ . Great improvement in percentage impedance bandwidth (IBW) is noticed by using a HWS over the single EWS. The proposed antenna possesses an IBW of 109.52% (3.66–12.52 GHz) whereas the antenna structure having only the EWS shows an IBW of only 23.40% (10.30–13.03 GHz). Merging of rectangular slots in a staircase fashion decreases the lower cutoff frequency from 10.30 to 3.66 GHz. Hence, miniaturization of 88.42% is achieved by using the HWS geometry. The gain of the proposed antenna varies from 1.65 to 5.8 dB along with average isolation of 26.72 dB in the entire operating frequency range. Compared to other reported wideband antennas, the proposed antenna achieves wide IBW, good gain within the operating frequency range with simple geometry and compact size of  $22 \times 24$  mm<sup>2</sup> only..

**Index Terms**— Microstrip-line-fed; compact; wideband; hybrid wideslot; staircase; impedance bandwidth.

## INTRODUCTION

Nowadays, more focussed efforts are being devoted to developing those antenna structures that can support multiple wireless standards and having compact dimensions for short-range and high-speed wireless applications. Microstrip antennas due to their low profile and low fabrication cost are best suited for such scenarios. However, their performance is affected by narrow impedance bandwidth (IBW) and low gain values. To mitigate these problems, several broadbanding techniques such as co-planar waveguide (CPW) [1]-[3], fractals [5]-[8] and defected ground structures [9]-[13] or a combination of them have been proposed in the literature.

Coplanar waveguide (CPW) antenna structures are highly popular for their wideband response [1]-[3]. In [1], a simple CPW-fed rectangular microstrip patch antenna (MSPA) is proposed which shows a wideband response (2.7–11.7 GHz). But the overall size of the antenna is large, i.e.,  $40 \times 52$  mm<sup>2</sup>. A large octagonal CPW-fed patch antenna of size  $47 \times 47$  mm<sup>2</sup> discussed in [2] shows large operating bandwidth of 7.5 GHz (2.0-9.5 GHz). But the proposed antenna shows a negative gain up to 5 GHz. A more compact CPW-fed circular MSPA with multiple circular slots in a stacked manner is proposed in [3]. Using a shape blending algorithm, an IBW of 30.5–80.1% can be achieved successfully as discussed in [4]. But low gain and large size are still major issues in the CPW-fed antennas. The self-similar and space-filling properties of fractals help antenna researchers to fabricate the antenna structures within highly restricted space [5]. To solve the compactness problem in MSPAs, several wideband fractal antennas in the last decade have been proposed [6]-[8]. In [6], a CPW-fed flower shaped circular fractal antenna is proposed that shows wideband characteristics from 2.6 to 13.46 GHz. A CPW-fed rectangular MSPA with '+' shaped fractal slots (up to 3 iterations) is discussed in [7]. But an IBW of only 56% (4.56-7.92 GHz) is obtained. In [8], a wideband Fibonacci spiral MSPA based on Koch curve is proposed. But due to the high design complexity of fractals, their modelling and fabrication are quite difficult. Microstrip-line-fed wide-slot antenna structures have several advantages including high impedance bandwidth, high gain and low cross-polarization over CPW and fractal counterparts [9]. An EWS antenna in multilayer scenario with a rotated

elliptical parasitic patch presented in [10] shows an IBW of 68.74%. Another similar structure but having an octagonal parasitic patch is proposed in [11] shows an IBW of 71.38%. A hexagonal wide-slot antenna having a circular slot at each corner is discussed in [12]. However, the proposed wide-slot structure shows the operating band from 2.16 to 3.43 GHz (45.19%) only. Recently, [13] came up with an idea of using multiple EWSs of different dimensions to produce a large IBW. Their proposed antenna shows the IBW ranging from 5.77-13.48 GHz.

This paper describes a compact and wideband microstripline-fed antenna by adding an elliptical wide-slot (EWS) and multiple rectangular slots in a staircase manner (named as hybrid wide-slot or simply HWS). Using the HWS, the proposed antenna shows the wideband behaviour ranging from 3.66 to 12.52 GHz. This paper is categorized as follows: Section-II presents various wideband antennas that are already published in the literature are discussed. In Section-III, the antenna design methodology using accurate design equations and steps to design the proposed antenna geometry are discussed. In Section-IV, both frequency and time-domain parameters are discussed. Finally, the applications of the proposed wideband antenna along with few concluding remarks are given in the conclusion section.

## ANTENNA DESIGN AND PROPOSED METHODOLOGY

### A. ANTENNA CONFIGURATION

The proposed wideband antenna consisting of EWS and four rectangular slots in staircase fashion is shown in Fig. 34-1. This HWS antenna is simulated using ANSYS Desktop ver. 17.0 on FR-4 material having dielectric constant ( $\epsilon_r$ ) 4.4, loss tangent ( $\tan\delta$ ) 0.02, and thickness ( $h$ ) 1.6 mm. It has HWS in the ground plane fed by an open-ended microstrip-line having a characteristic impedance of  $50\Omega$ .

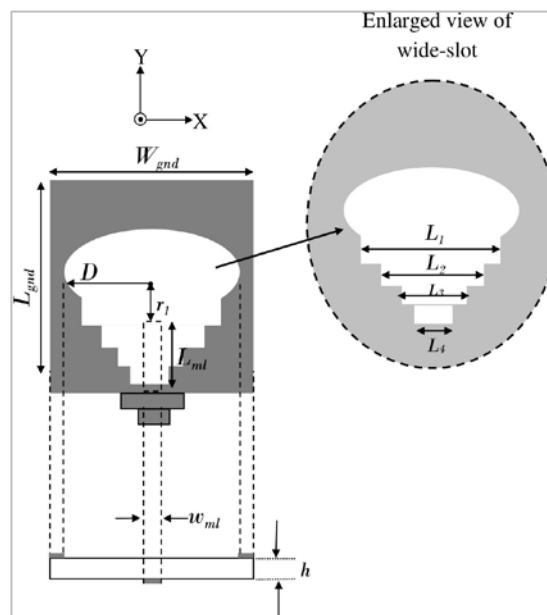


Figure 34-1 Schematic of the proposed hybrid wide-slot antenna fed by  $50\Omega$  microstrip line.

The distance between the open end of the microstrip-line and centre of the EWS is known as *feeding distance* ( $r_1$ ). The relationship between the input impedance of an EWS and  $r_1$  is given by [14]

$$R_{in}(r_1) = \frac{1}{G_{T,mn}} \frac{J_1^2(kr_1)}{J_1^2(kD)} \quad (1)$$

where  $k$  is the propagation constant,  $\frac{1}{G_{T, nm}}$  is the input impedance of the  $TM_{mn}$  mode and depends on  $m^{th}$  zero of the Bessel function of order  $n$ . The parameter  $kD=1.84$  refers to the fundamental mode. The value of  $G_{T, mn}$  can be determined by [14]

$$G_{T, mn} = G_{ohmic} + G_{diel} + G_{rad} \quad (2)$$

where  $G_{ohmic}$ ,  $G_{diel}$ , and  $G_{rad}$  are referred to as conductance due to ohmic, dielectric, and radiation loss respectively and are given in [14]. The value of  $r_1$  is varied to obtain a good level of matching over a large frequency range as shown in Fig. 34-2.

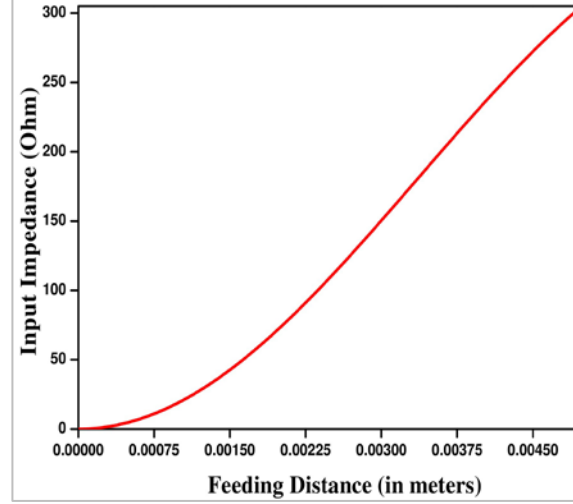


Figure 34-2 Input impedance  $R_{in}(r_1)$  variation with feeding distance  $r_1$ .

The design evolution of the proposed HWS antenna starts with the designing of an elliptical slot excited by a microstripline of characteristic impedance  $50\Omega$ . The relationship between the size of an EWS and its frequency of operation for dominant mode  $TM_{11}$  is given by [15]

$$f_{11}^{e,o} = \frac{15}{\pi e \cdot D} \sqrt{\frac{q_{11}^{e,o}}{\epsilon_r}} \text{ GHz} \quad (3)$$

where  $D$  is the length of the semi-major axis of the EWS having eccentricity  $e$  and  $q_{11}^{e,o}$  is an approximated Mathieu function for even  $q_{11}^e$  and odd mode  $q_{11}^o$  which is given by [15]

$$q_{11}^e = -0.0049e + 3.7888e^2 - 0.7228e^3 + 2.2314e^4 \quad (4a)$$

$$q_{11}^o = -0.0063e + 3.8316e^2 - 1.1351e^3 + 5.2229e^4 \quad (4b)$$

## B. DESIGN STEPS

The evolution procedure of the proposed wideband antenna is illustrated in Fig. 34-3(a). Initially, an EWS is etched from the ground plane which is excited with the help of  $50\Omega$  microstrip-line [Ant 1]. The major constraint while designing a wide-slot antenna is that the overall size of the antenna is governed by the size of the wide-slot. To overcome this issue, an EWS of smaller dimension is etched and afterwards, multiple rectangular slots in staircase fashion are etched from the ground plane. The size of the EWS and feeding distance  $r_1$  are varied to obtain a good matching across the large frequency band. Ant 1 provides an IBW of 23.40% (10.3013.03 GHz) as shown in Fig. 34-3(b). To shift this frequency band towards the lower edge, multiple rectangular slots are etched in successive stages, i.e., up to Ant 5 which is the final proposed antenna geometry. The addition of rectangular slots decreases the lower cutoff frequency and creates a lower frequency band [Ant 3]. This lower-frequency merges with the upper-frequency band with successive addition of rectangular slots [Ant 4]. By using these slots, the lower cutoff frequency gets shifted from 10.30 to 3.66 GHz, i.e., miniaturization of 88.42% has been achieved.

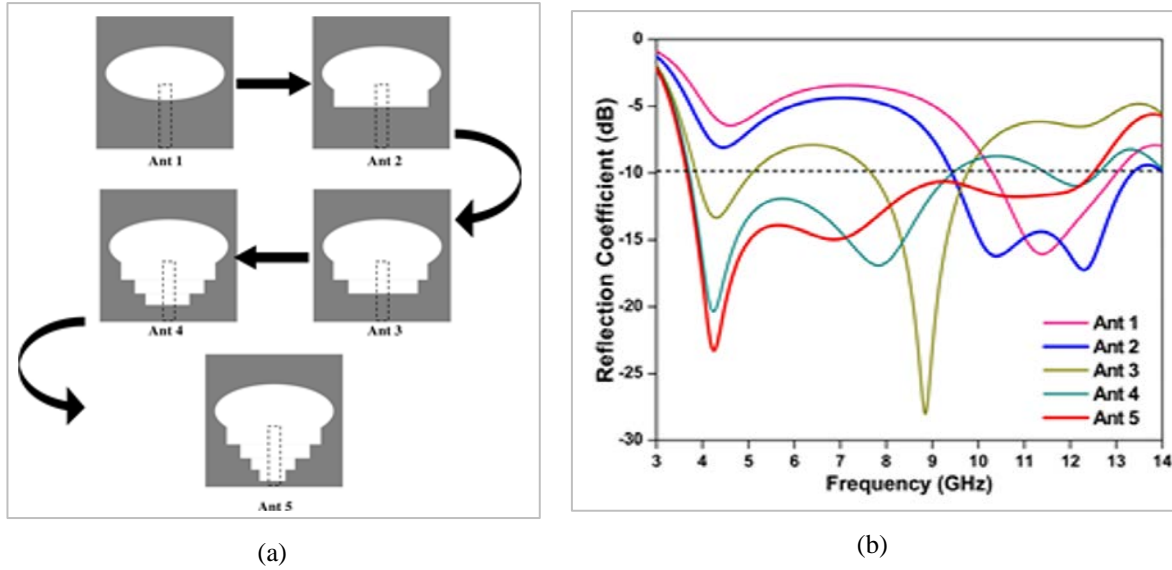


Figure 34-3 (a) Reflection coefficient and (b) impedance versus frequency for the proposed wideband antenna

### RESULTS AND DISCUSSION

The frequency domain parameters such as  $S$ -parameters, surface current distributions, impedance, gain, and radiation patterns are discussed in the following subsections. Time domain parameters including group delay and transfer function are also discussed.

#### A. FREQUENCY-DOMAIN PARAMETERS

##### *Reflection coefficient and impedance versus frequency:*

The simulated reflection coefficient ( $S_{11}$ ) of the proposed antenna is shown in Fig. 34-4(a) which is one of the key parameters for describing the operating bands. It is observed that the proposed antenna shows wideband behaviour ranging from 3.66–12.52 GHz which covers both C and X-bands, hence suitable for wireless applications that operate in this frequency range. Fig. 34-4(b) shows the real and imaginary parts of the impedance which should be ideally 50 and 0Ω, respectively. It is clear that both imaginary and real parts of the impedance oscillate around 0 and 50Ω within the operating frequency band, respectively.

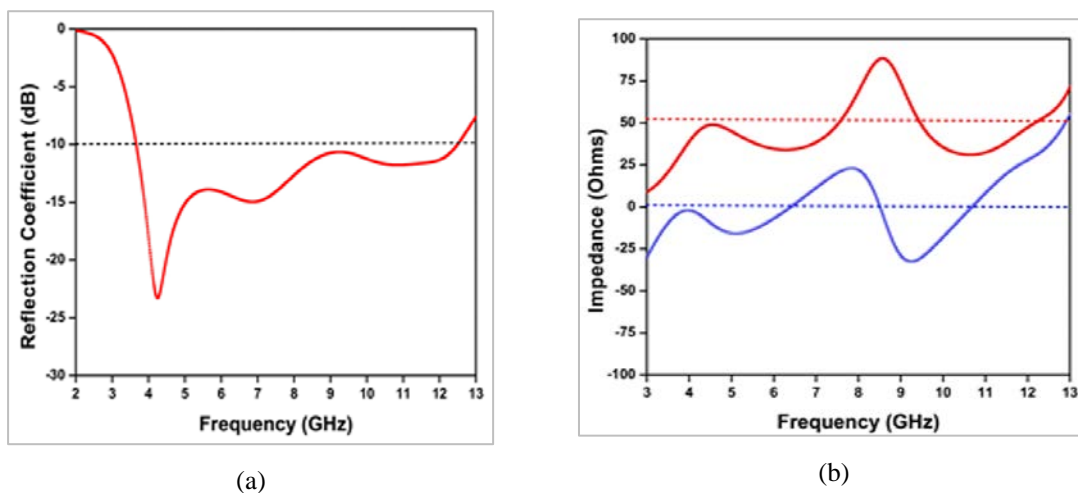


Figure 34-4 (a) Reflection coefficient and (b) impedance versus frequency for the proposed wideband antenna

**Surface current distribution:**

Fig. 34-5 shows the surface current distribution at different resonating frequencies. At lower frequency, i.e., 4.25 GHz (as shown in Fig. 34-5(a)), the surface current is mainly concentrated near the lowermost rectangular slot. At 6.86 GHz frequency, the surface current starts concentrating near the EWS periphery (shown in Fig. 5(b)). At higher frequencies, i.e., 10.85 GHz, the surface current is focussed near the EWS and staircase slots (shown in Fig. 34-5(c)).

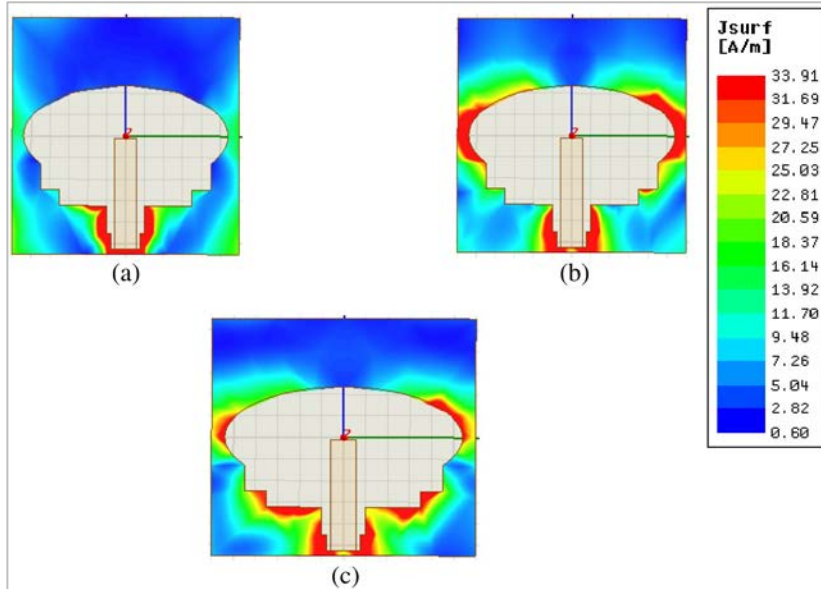


Figure 34-5 Surface current distribution at (a) 4.25, (b) 6.86 and (c) 10.85 GHz.

**Gain versus frequency:**

Fig. 34-6 shows the simulated gain curve for the proposed antenna within the operating frequency range. From Fig. 6, it can be studied that the co-polarization (CP) and cross-polarization (XP) gain of the antenna varies from 1.65 to 5.80 dB and from -36.75 to 8.20 dB, respectively. The average value for CP and XP gain is 3.63 and -23.09 dB, respectively. Hence, a good level of isolation ranging from 12.86 to 39.27 dB is reported for the proposed wideband antenna.

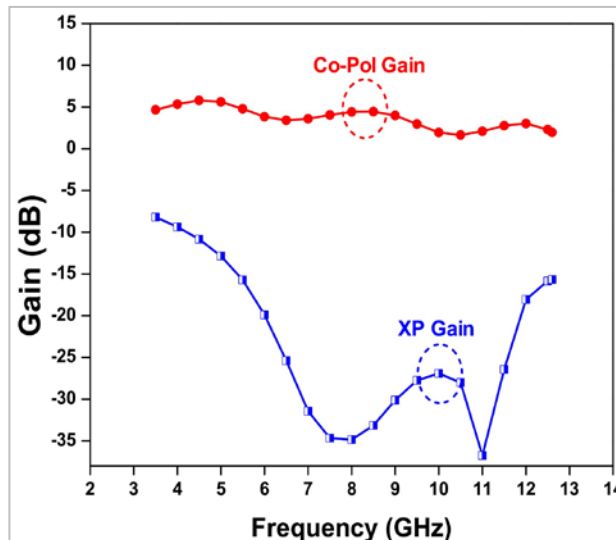


Figure 34-6 . Variaiton in co-polarized and cross-polarized (XP) gain with frequency

**Radiation pattern:**

The radiation pattern of the proposed wideband antenna at 4.25, 6.86 and 10.85 GHz is depicted in Fig. 34-7(a), 34-7(b) and 34-7(c), respectively. An isolation of 15.67, 33.29 and 33.86 dB is obtained at 4.25, 6.86 and 10.85 GHz, respectively. The back radiation due to the presence of HWS leads to the near omnidirectional radiation pattern at a lower frequency. However, at a higher frequency, a little deviation can be observed which may be due to the excitation of high order resonating mode.

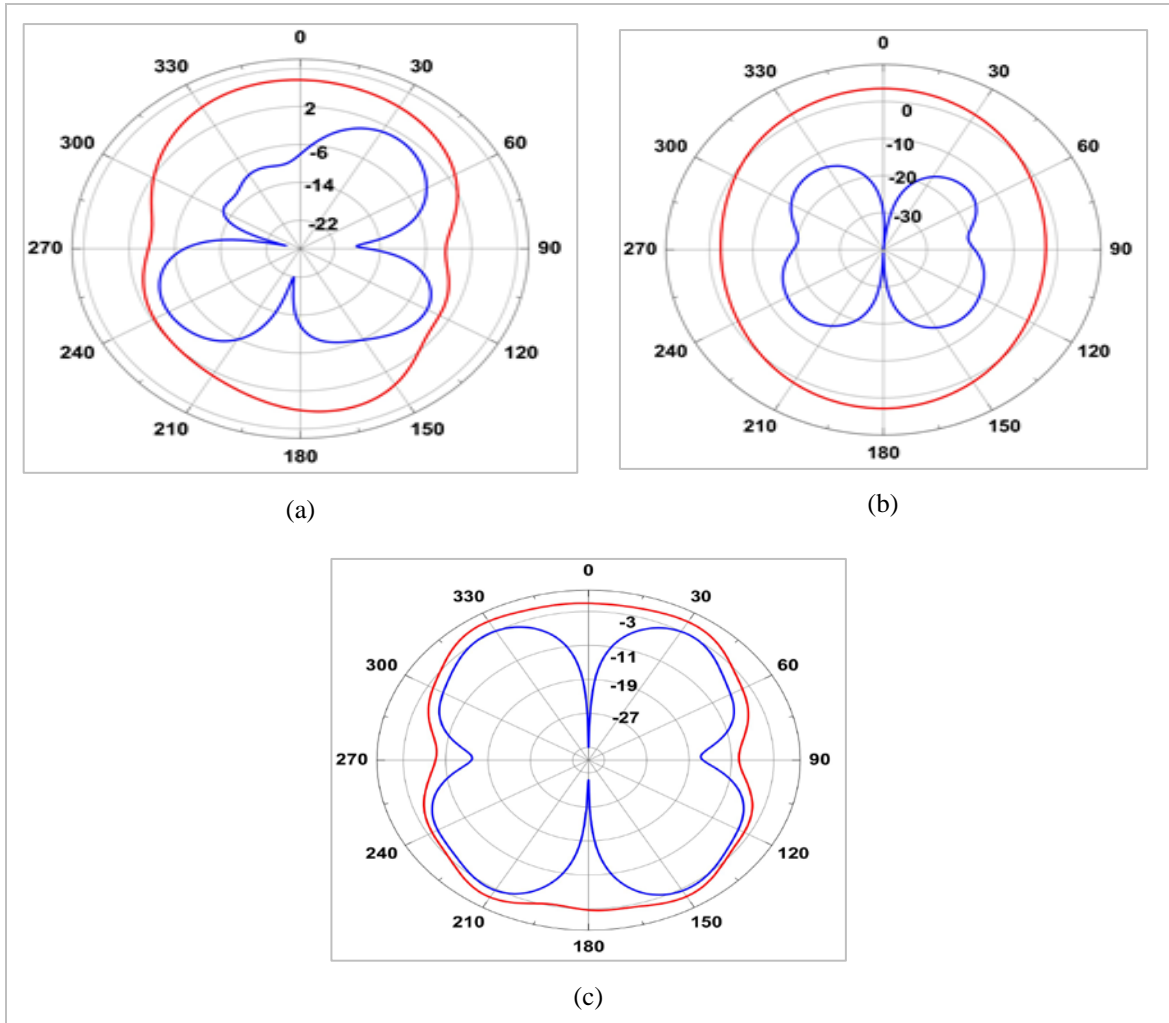


Figure 34-7 Simulated 2D radiation pattern at (a) 4.25 GHz, (b) 6.86 GHz and (c) 10.85 GHz. Solid red line: co-polarization and solid blue line: crosspolarization

**B. TIME-DOMAIN PARAMETERS**

In the previous subsection, the performance of the proposed antenna in frequency-domain has been analyzed. The good performance in frequency-domain cannot guarantee that the given antenna will behave well in time-domain as well. For this, time-domain analysis using group delay parameter has been performed.

**Group-delay:**

The group delay of the proposed antenna for side-by-side (SS) configuration is shown in Fig. 34-8(a). It is clear that the group delay for SS configuration is below 1 ns within the operating frequency range which is a prime requirement for the wideband applications.

**Transfer characteristics:**

The transfer function ( $S_{21}$ ) and phase response ( $\angle S_{21}$ ) of the proposed antenna are depicted in Fig. 34-8(b). For better time-domain response, the  $S_{21}$  should be below -20 dB and phase response should vary linearly. From Fig. 8(b) it is clear that both  $S_{21}$  and phase response are within their desired limits in the range where reflection coefficient is below -10 dB.

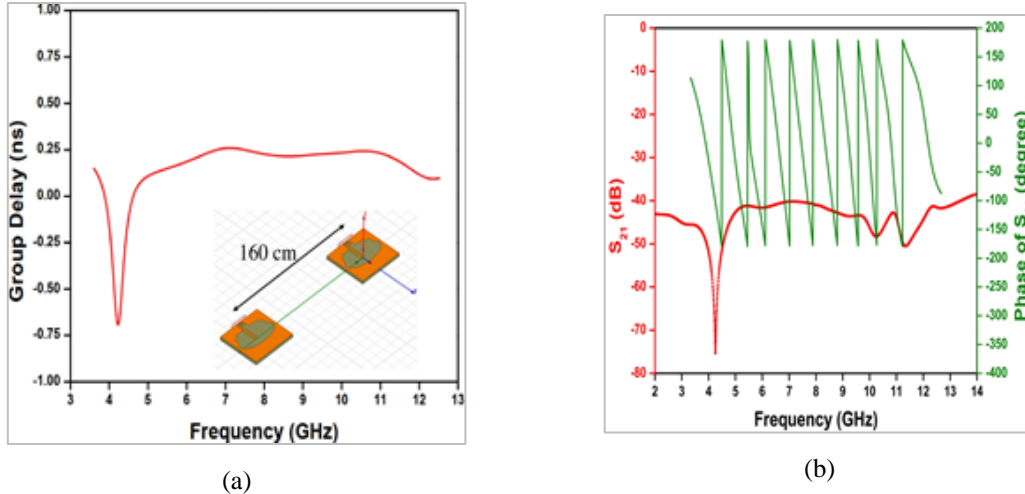


Figure 34-8. (a) Group delay and (b)  $S_{21}$

**C. COMPARISON WITH EARLIER REPORTED ANTENNA STRUCTURES**

Since the frequency of operation and size of the antennas discussed in this paper are different hence, a parameter known as bandwidth-dimension-ratio (BDR) is calculated and compared with the proposed antenna.

$$BDR = \frac{\%B.W.}{\lambda_W \times \lambda_L(5)}$$

where  $\lambda_W \times \lambda_L$  is the electrical dimension of the antenna.

Table 34-1 shows the comparison of the proposed antenna with the antenna structures discussed in Section-I (“Introduction”). It is observed that the proposed wide-slot antenna has the highest BDR of about 1393 among all the reported antenna structures.

Table 34-1 COMPARISON OF PROPOSED HWS ANTENNA WITH EARLIER REPORTED WIDEBAND ANTENNAS

Ref./Year	Physical size (WGND×LGND mm2)	Electrical Size ( $\lambda_W \times \lambda_L$ )	Frequency range (GHz)	Peak gain (dB)	BDR (= $\frac{\%B.W.}{\lambda_W \times \lambda_L}$ )	Technique used
[1]/2018	40×52	0.36×0.47	2.7-11.7	-	741.93	CPW rectangular MSPA
[2]/2018	47×47	0.31×0.31	2.0-9.5	3.5	1328.56	CPW-fed octagonal ring MSPA
[3]/2018	36×45	0.38×0.48	3.2-13.9	<8	678.96	CPW-fed slotted circular MSPA
[6]/2013	43×51	0.35×0.42	2.46-13.46	7.1	937.16	Circular fractal MSPA
[7]/2017	30.6×30.6	0.47×0.47	4.56-7.92	-	248.9	‘+’ shaped fractal
[8]/2018	18×35	0.39×0.48	2.34-11.5	-	713.35	Koch curve fractal
[10]/2017	25×24	0.32×0.30	3.8-7.78	11	714.05	EWS+multilayer
[11]/2018	25×24	0.33×0.32	4.0-8.44	10.3	669.21	EWS+multilayer
[12]/2018	40×40	0.29×0.29	2.16-3.43	2.6(avg.)	543.57	Hexagonal wide-slot
[13]/2019	22×24	0.42×0.46	5.77-13.48	8.66	410.12	Multiple asymmetric EWS
This work	22×24	0.26×0.29	3.66-12.52	5.8	1393.58	HWS antenna

## CONCLUSION

An idea of merging different shapes for enhancing the impedance bandwidth is presented in this paper. Two different shapes, i.e., ellipse and rectangle in the form of staircase manner are merged with each other which give a wideband response ranging from 3.66 to 12.52 GHz (or 109.52%). The presence of rectangular slots in staircase fashion reduces the lower cutoff frequency from 10.30 to 3.66 GHz, thereby leading to miniaturization of 88.42%. A peak gain of 5.79 dB and a good level of isolation (below 15 dB) within the operating frequency band is obtained. A group delay of below 1 ns and linear phase response ensure the applicability of the proposed antenna for wideband wireless applications. The compact dimensions of  $22 \times 24 \text{ mm}^2$  (or  $0.26\lambda_o \times 0.29\lambda_o$  where  $\lambda_o$  is the wavelength corresponding to lowest cutoff frequency, i.e., 3.66 GHz). All these features make the proposed HWS antenna a good candidate for modern wireless applications such as wireless LANs (upper band: 5.72–5.82 GHz), communication satellites (C-band) and military applications (X-band).

## REFERENCES

- [1] S. Peddakrishna and T. Khan, "Design of UWB monopole antenna with dual notched band characteristics by using  $\pi$ -shaped slot and EBG resonator," *AEU-International Journal of Electronics and Communications*, vol. 96, pp. 107-112, Nov. 2018.
- [2] P. Khanna, A. Sharma, A. K. Singh, and A. Kumar, "A CPW-fed octagonal ring shaped wide band antenna for wireless applications," *Advanced Electromagnetics*, vol. 7, no. 3, Aug. 2018.
- [3] K. Srivastava, A. Kumar, B. K. Kanaujia, and S. Dwari, "Integrated amateur band and ultra-wide band monopole antenna with multiple bandnotched," *International Journal of Electronics*, vol. 105, no. 5, pp. 741755, 2018.
- [4] A. Wu, Z. Zhang and B. Guan, "A shape blending based design of printed slot antennas for various wideband applications," *Microwave and Optical Technology Letters*, vol. 61, pp. 374-380, 2019, DOI: 10.1002/mop.31572
- [5] M. Kumar and V. Nath, "Introducing multiband and wideband microstrip patch antennas using fractal geometries: Development in Last decade," *Wireless Personal Communications*, vol. 98, no. 2, pp. 2079-2105, Jan. 2018, DOI: 10.1007/s11277-017-4965-x
- [6] D. J. Kim, J. H. Choi and Y. S. Kim, "CPW-fed ultrawideband flower-shaped circular fractal antenna," *Microwave and Optical Technology Letters*, vol. 55, no. 8, pp. 1792-1795, 2013.
- [7] S. Kakkar and S. Rani, "Implementation of fractal geometry to enhance the bandwidth of CPW fed printed monopole antenna," *IETE Journal of Research*, vol. 63, no. 1, pp. 23-30, 2017.
- [8] C. Sharma and D. K. Vishwakarma, "Miniaturization of Spiral Antenna Based on Fibonacci Sequence Using Modified Koch Curve," *IEEE Antennas and Wireless Propagation Letters*, vol. 16, pp. 932-935, 2017.
- [9] M. Kumar and V. Nath, "Microstrip-line-fed elliptical wide-slot antenna with similar parasitic patch for multiband applications," *IET Microwaves, Antennas & Propagation*, vol. 12, no. 4, pp. 2172-2178, Nov. 2018, DOI: 10.1049/iet-map.2018.5377
- [10] M. Kumar and V. Nath, "Improved cross polarization and wideband multilayer wide-slot microstrip antenna with rotated parasitic patch," 2017 IEEE Asia Pacific Microwave Conference (APMC), Kuala Lumpur, pp. 964-967, 2017, DOI: 10.1109/APMC.2017.8251611
- [11] M. Kumar and V. Nath, "Dual-Band Dual-Polarized Stacked Octagonal Fractal Patch Antenna with Nonlinear Manipulation," 2018 IEEE Radio and Antenna Days of the Indian Ocean (RADIO), Grand Port, 2018, pp. 1-4, DOI: 10.23919/RADIO.2018.8572374
- [12] S. P. Gangwar, K. Gangwar and A. Kumar, "A compact modified hexagonal slot antenna for wideband applications," *Electromagnetics*, vol. 38, no. 6, pp. 339-351, 2018.
- [13] M. Kumar and V. Nath, "Open Ended Microstrip-line-fed Compact Wideband MIMO-Diversity Antenna with Multiple Asymmetric Elliptical Wide-Slots," 2019 URSI Asia-Pacific Radio Science Conference (APRASC), New Delhi, India, pp. 1-4, 2019, DOI: 10.23919/URSIAPRASC.2019.8738508
- [14] F. Abboud, J. P. Damiano and A. Papiernik, "A new model for calculating the input impedance of coax-fed circular microstrip antennas with and without air gaps," *IEEE Trans. Ant. Propag.*, vol. 38, no. 11, pp. 1882-1885, 1990.
- [15] J. G. Kretzschmar, "Wave propagation in hollow conducting elliptical waveguides," *IEEE Trans. Microw. Th. Tech.*, vol. 18, no. 9, pp. 547-554, 1970.